LOCAL LUNAR TOPOGRAPHY FROM THE APOLLO 17 ALSE RADAR IMAGERY AND ALTIMETRY

C. ELACHI, M. KOBRICK, L. ROTH, M. TIERNAN, and W. E. BROWN, Jr.
Space Sciences Division, Jet Propulsion Laboratory, California Institute of Technology, Pasadena, Calif., U.S.A.

(Received 19 September, 1975)

Abstract. The Apollo 17 ALSE VHF radar provided imagery and continuous profiling data around the Moon during two revolutions. The imagery data are used to derive depth and diameter measurements of small craters (diameter <30 km). The profiling data are used to study the topography of a few large craters: the bulged floors in Hevelius, Neper, and Aitken; central peaks in Neper and Buisson; and the depressed floor of Maraldi. The same data provided accurate (better than 25 m) profiles of Mare Crisium and Mare Serenitatis.

1. Introduction

One of the scientific instruments carried by the Apollo 17 Service Module was a radar sounder (ALSE, Apollo Lunar Sounder Experiment) (Brown, 1972; Porcello *et al.*, 1974). This sensor operated at three frequencies (5, 15, and 150 MHz) in a coherent synthetic aperture mode; thus both sounding and high-resolution imagery were obtained. The data to be discussed in this paper are preliminary results derived from the VHF (150 MHz) imagery, which was obtained during revolutions 24, 25, and 26 of the Command-Service Module (two complete orbits), and part of Rev. 73. Similar processing and analysis is now underway for all areas overflown while the radar was operating, and will be published at a future date.

The radar imagery corresponds to a 30 km wide swath taken continuously independent of solar illumination (since the radar is an active system). In this paper we use some of this imagery to: (1) determine the depth and diameter of a number of small craters (diameter <30 km) and compare some of them to the most recent available measurement derived from lunar photographs (Arthur, 1974); (2) derive accurate topographic profiles of a few large craters and study their morphology and its implication on the formation of these craters; and (3) determine the profiles of Maria Crisium, Tranquillitatis, and Serenitatis.

All the profiles have been corrected to remove the apparent slope caused by the spacecraft orbital eccentricity and are referenced to a sphere centered on the lunar center of mass, so that surfaces of constant elevation would appear as straight lines in the figures. The profiles have been compared to the results from adjacent orbits of the Apollo 17 Laser Altimeter (Kaula *et al.*, 1974), which give absolute elevations at intervals of 30 km. The results are consistent within the limits of the spacecraft ephemeris. The inherent accuracy of the radar system is about 25 m.

The Moon **15** (1976) 119–131.

2. Geometry of the Radar Imagery

The ALSE viewing angle was such that profiling data were obtained simultaneously with the VHF imagery. The profile is a simple direct measurement of the time delay of the leading edge of the echo. Thus a continuous measurement of the spacecraft-surface distance was obtained over two orbits. The rest of the echo, which corresponds to reflections and scattering from off-track targets, contains the imagery information. In the cross-track dimension, the radar measures the time delay to a specific feature, i.e., its range. In the along-track dimension, the radar determines the viewing angle by measuring the Doppler history. Thus the radar imagery is in a distance-distance format rather than the angle-angle format of photographic imagery. This geometry leads to the type of distortion shown in Figures 1 and 2. Craters would look elliptical or circular depending on their positions in the swath. Most of the small-size craters look like a tear drop because the far-range rim is closer to the spacecraft than the

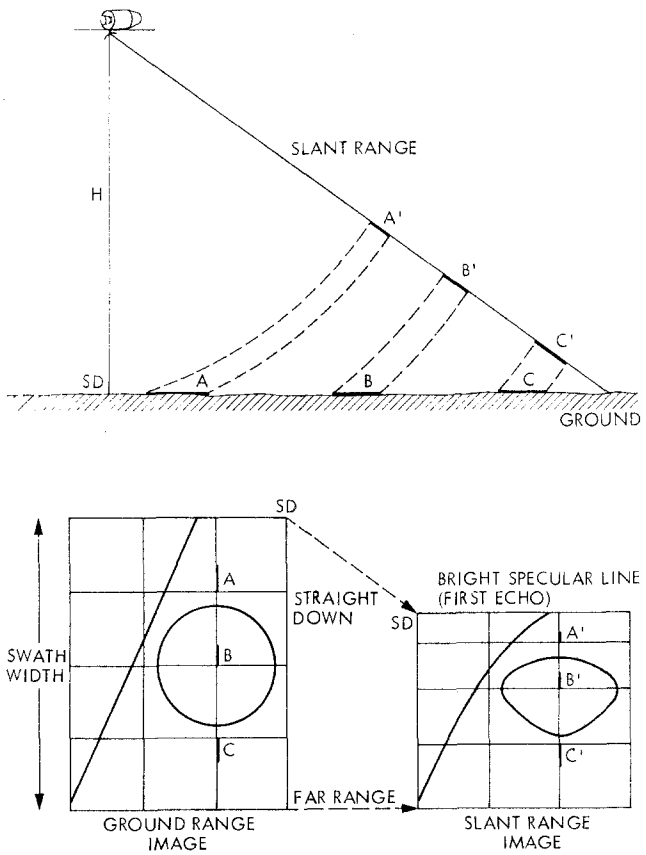

Fig. 1. Radar geometry across the line of trajectory (trajectory perpendicular to the plane of the page). The radar image covers a swath from straight down out to about 40 km to the right. The inherent geometric distortion in the radar image is shown in the lower sketches.

bottom. All the imagery shown in this paper contains this distortion. However, the measurements reported are all corrected to give actual height, depth, and size. It should be emphasized that this geometric distortion affects only the imagery and not the profile.

The major source of error in the profile determination is the spacecraft orbit. The uncertainty in the absolute radial position of the spacecraft is of the order of several hundred meters, but the relative uncertainty over the short intervals discussed in this

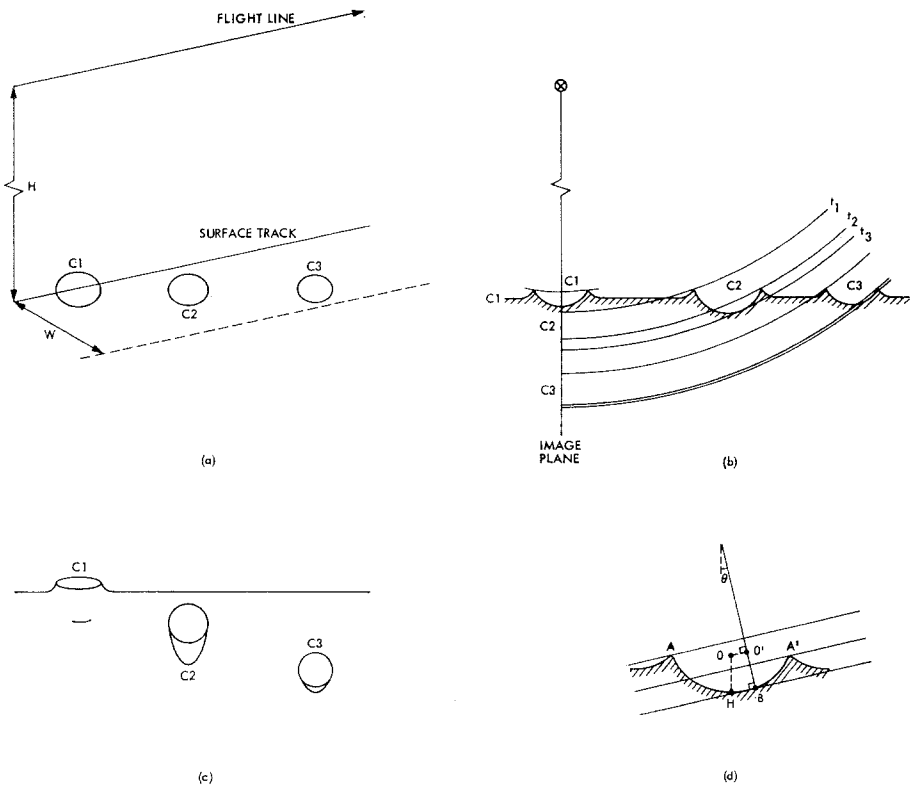

Fig. 2. Geometric distortion in the imagery of craters: (a) three identical craters are chosen as different positions in the swath. (b) Equi-distance circulars illustrate the geometric distortion which is sketched in (c). (d) Geometry used to determine the crater depth (see text).

paper, or between adjacent orbital tracks, is less than 100 m. Since the VHF imagery has not yet been used to determine absolute elevations only relative profiles are presented here, and therefore have a maximum relative error of less than 100 m.

Another error source in the profile measurement is the possibility that the first return is not from the subspacecraft point but from some off-track target. This effect is minimized in the present work since we are considering profiles of only relative smooth mare surfaces and the interior of filled craters.

3. Depth and Diameter of Small Craters

A typical radar image of a small crater is shown in Figure 3. The depth and diameter of 23 small craters (diameter <30 km) along and near the tracks of Revolutions 24, 25, 26 and part of 73 were measured. The diameter measurement for a circular crater is straightforward (Figure 2d). The along-track scale on the image is related to the surface dimensions through the spacecraft velocity and the running speed of the radar signal film. This scale varied from 1.0 km mm^{-1} to about 1.2 km mm^{-1}, depending on the position of the spacecraft in its near-circular orbit. The main error in the diameter measurement is in the location of the rim. We assumed it to be the inside edge of the bright line. The actual measurement error is less than 0.1 mm (i.e., $\simeq 100$ m), leading to a relative measurement error of about 6% for the smallest crater to less than 1% for the largest crater.

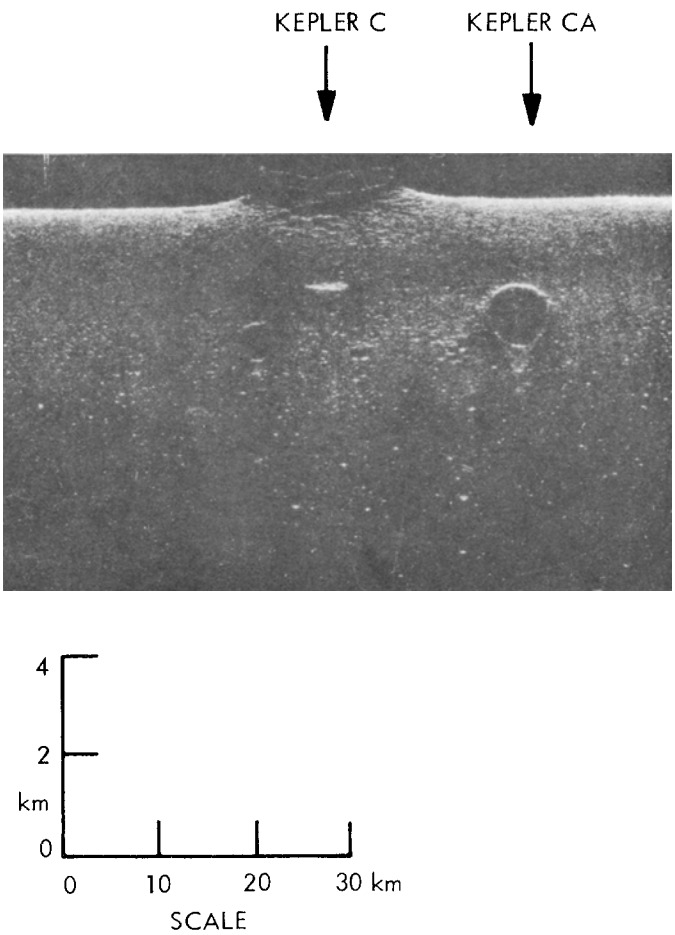

Fig. 3. Typical example of a small crater (Kepler C) which was straight under the Apollo 17 orbit. Kepler CA illustrates the distortion discussed in the previous figure.

The depth measurement is slightly more involved. In the case where the spacecraft flew directly over the crater (Figure 3), the depth measurement is straightforward: the distance measured is between the highest point on the rim and the crater bottom. The scale is 210 m mm^{-1} and our measurement accuracy is better than 25 m. In the case where the crater was to the side of the spacecraft, the depth was determined in the following way (see Figure 2d):

(1) The center 0 of the crater was taken as the middle of the azimuth line, which joins the farthest points (A, A') on the rim of the crater.

(2) The distance $0'B$ was measured.

TABLE I

Small crater D, d measurements (in meters)

Crater	Radar			Photo (Arthur, 1974)		
	D_r	d_r	d_r/D_r	D_p	d_p	d_p/D_p
Aratus	8100	1155	0.14			
Bessel E	6500	1360	0.21	6500	1230	0.19
Desseillingy	6700	1344	0.20	6550	1190	0.18
Next to Desseillingy	2570	567	0.22			
	2000	400	0.20			
Draper C	7826	1870	0.24	7790	1620	0.21
Eratosthenes A	6700	1218	0.18	6480	1250	0.19
Eratosthenes B	6037	1239	0.21	5890	1110	0.19
Huygens A	7372	1200	0.16	7750	930	0.12
Jansen (C)	8400	1260	0.15	8450	1000	0.18
Kepler C	13416	2058	0.15	12240	2170	0.18
Kepler CA	5366	1071	0.20	5460	960	0.18
After Kepler C	4000	670	0.17			
Macrobius A	22470	3780	0.17	20060	3640	0.18
Marius DA	4360	924	0.21			
Next to Marius	2460	588	0.24			
Maraldi A	7820	1060	0.16			
Riccioli CA	17458	3780	0.21			
Sulpicius Gallus	11850	2330	0.20	12170	2160	0.18
Next to Sulpicius Gallus	1700	300	0.18			
West edge of Crisium	3800	840	0.22			
East edge of Crisium	3900	705	0.18			

As shown in Figure 2d, $0'B$ is not actually the height. B is the point on the inside of the crater, which is the farthest away from the spacecraft. However, as the range look angle θ of all the craters measured is less than 17°, we can assume that the depth $d \simeq 0'B \cos\theta$ or $d \simeq 0'B$ with an error less than 5%.

The results of our data are summarized in Table I and compared to the measurements of Arthur (1974). We found that our depth measurements are fairly consistent with previous measurements. The best calibration is obtained by considering the craters which were straight under the Apollo 17 orbit and for which the depth measurements are direct and most accurate. Sulpicius Gallus and Kepler C craters fall

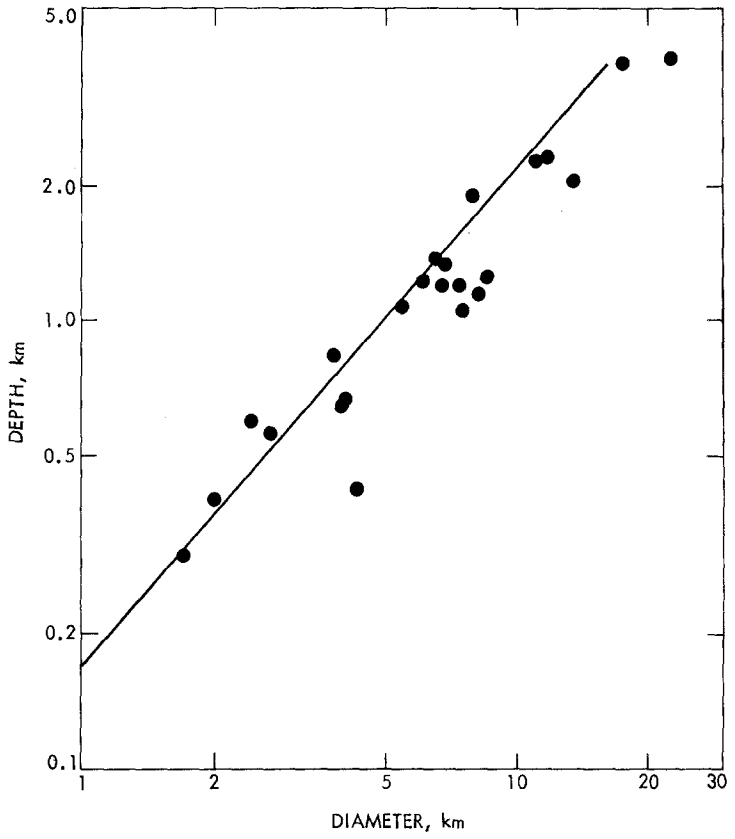

Fig. 4. Craters depth d vs diameter D as derived from the radar measurements. The straight line corresponds to $d=0.2\ D$.

in this category:

Sulpicius Gallus: radar depth = 2330 m vs 2160 m (6% difference)
Kepler C: radar depth = 2058 m vs 2170 m (5% difference)

Our measurements were also plotted on a depth-diameter ($d-D$) graph (Figure 4), and they fitted well with the curve derived by Pike (1974) from photographic imagery of small craters (diameter $\leqslant 15$ km):

$$d \simeq 0.2\ D,$$

where D is the rim-to-rim diameter (km), and d is the crater depth (km).

4. Large Craters Profiles

Apollo 17 overflew a number of large craters (diameter $\gtrsim 30$ km) during Revolutions 24, 25, and 26, and the radar imagery was able to provide accurate profiles for each of them by the method discussed in Section 2. Profiles are now being prepared for all

craters overflown while the radar was operating; some preliminary results are presented here for two large (Hevelius and Neper) and two smaller (Maraldi and Buisson) craters.

Hevelius has a rim-to-rim diameter of approximately 110 km and Neper approximately 140 km, and the two are situated in somewhat different geological provinces.

Hevelius is located in the terra region on the edge of the Procellarum-Imbrium system; Neper is in the isthmus separating Mare Smythii from Mare Marginis. Both of them show floor doming, which was profiled with the ALSE radar to an accuracy of better than 25m. In this section we present the profiles and discuss their implications for the above craters and for Maraldi and Buisson. Note that Figures 5 through 8 are oriented with east to the left, and north downward.

The Hevelius profile (Figure 5) was recorded along the diagonal suborbit track from lunar coordinates (69°33′W, 0°57′N) to (65°12′W, 2°31′N) during orbit 26. The main feature in the profile is the central bulge. We remark that: (1) the bulge has a maximum height of 325 m; (2) the bulge peak is shifted by about 4 km from the crater center, away from Oceanus Procellarum; and (3) the average crater floor is

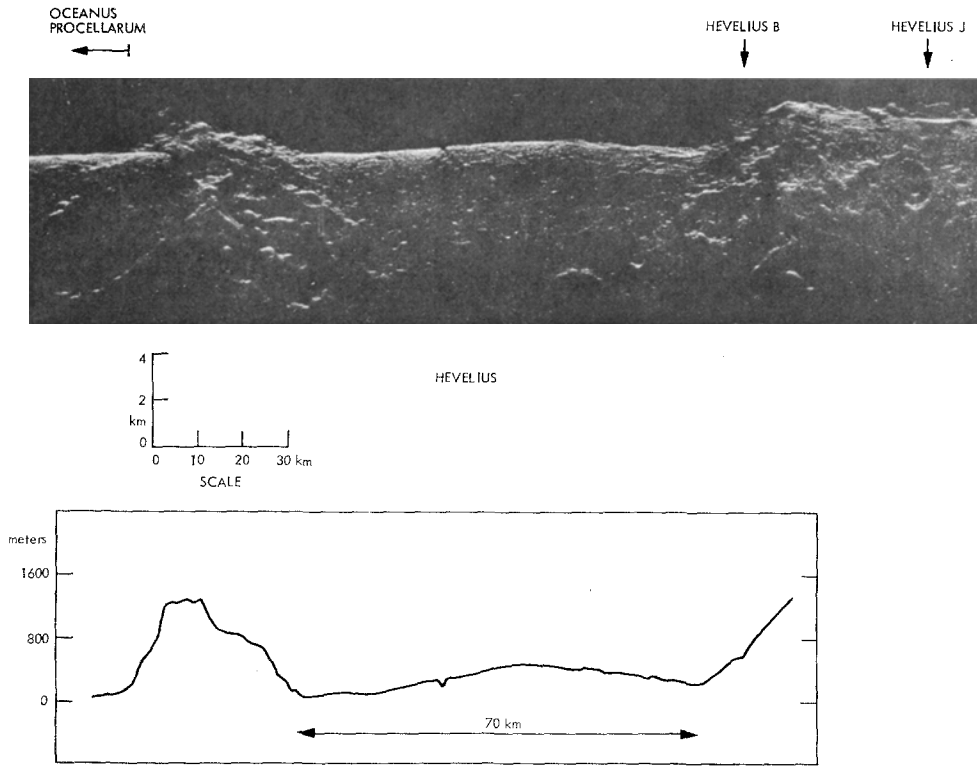

Fig. 5. Radar image and profile of Hevelius. Note that the east is to the left and the north is down in the image. Note also the difference in the scales. The vertical scale should only be applied to the profile and not to the cross track surface dimensions.

tilted by about 200 m over a distance of 70 km toward the eastern rim, such that the eastern floor is at exactly the same level as Procellarum.

Hevelius is a smaller version of a Humboldt-type crater (Baldwin, 1968) with a lava-filled floor. The updomed floor exhibits largely radial fracture patterns. It has been speculated that the fracture pattern is a consequence of the process of isostatic compensation, during which the wall of the crater sinks and the floor rises. Quoting Baldwin, "The floor rose, but, before it had reached the flat-floor stage, the floor was partially covered with lava which came from below. This lava was thicker in the central regions around the central peak. The lava floor then solidified. Its superimposed weight was not sufficient to stop the isostatic adjustment, and the floor continued to arch upward and the fracture pattern appeared." The doming apparent in the radar profile is consistent with this hypothesis.

The Hevelius profile deserves attention for one more reason. Baldwin (1971) has noticed that the average elevation of the lunar continental surface diminishes as the mare shore is approached. The drop in the average elevation continues deep into the mare away from the shore; the drop is approximately $\frac{1}{2}$ km at a distance 150 km from the shore. The phenomenon is a likely consequence of the mare floor sinking under the weight of the superimposed lava. The Hevelius profile provides support of this hypothesis. The difference in elevation between the crater floor levels closest to Procellarum and farthest away from it is approximately 200 m over a distance of 70 km, in accordance with the Baldwin observation.

The Neper profile (Figure 6) is also across the center of the crater. The ephemeris coordinates of the suborbit track are (89° E, 6° 52′ N) to (80° 46′ E, 9° 48′ N), orbit 25. The Neper floor shows similar arching (325 m) when compared to Hevelius and the same average slope (325 m over 116 km) toward the southeast.

A major feature of Neper is the central peak, which was measured to be 1475 m above the lava floor. Using the relation given by Wood (1973), which relates the central peak height h to the crater diameter D by

$$h \simeq 0.026\, D - 0.26\,,$$

we find that h would be $\simeq 3.38$ km. This implies that the lava thickness near the center is about 1.9 km. However, if we use Pike's relation (Pike, 1974) between the crater diameter D and depth d of large craters – i.e.,

$$d \simeq D^{0.3}\,,$$

we find that predicted depth would be 4.4 km, leading to a lava thickness of roughly 1.0 km at the crater center.

In addition to Hevelius and Neper, a short (≈ 30 km) pass near the southern edge of the farside filled crater Aitken (diameter ≈ 140 km) has been studied; the first indications are that doming similar to that found in Neper is present.

A sample of three examples does not allow one to make general conclusions about all lunar craters of comparable size. Yet it is certaintly a conspicuous coincidence that all three observed craters of the size class in question show a pronounced floor

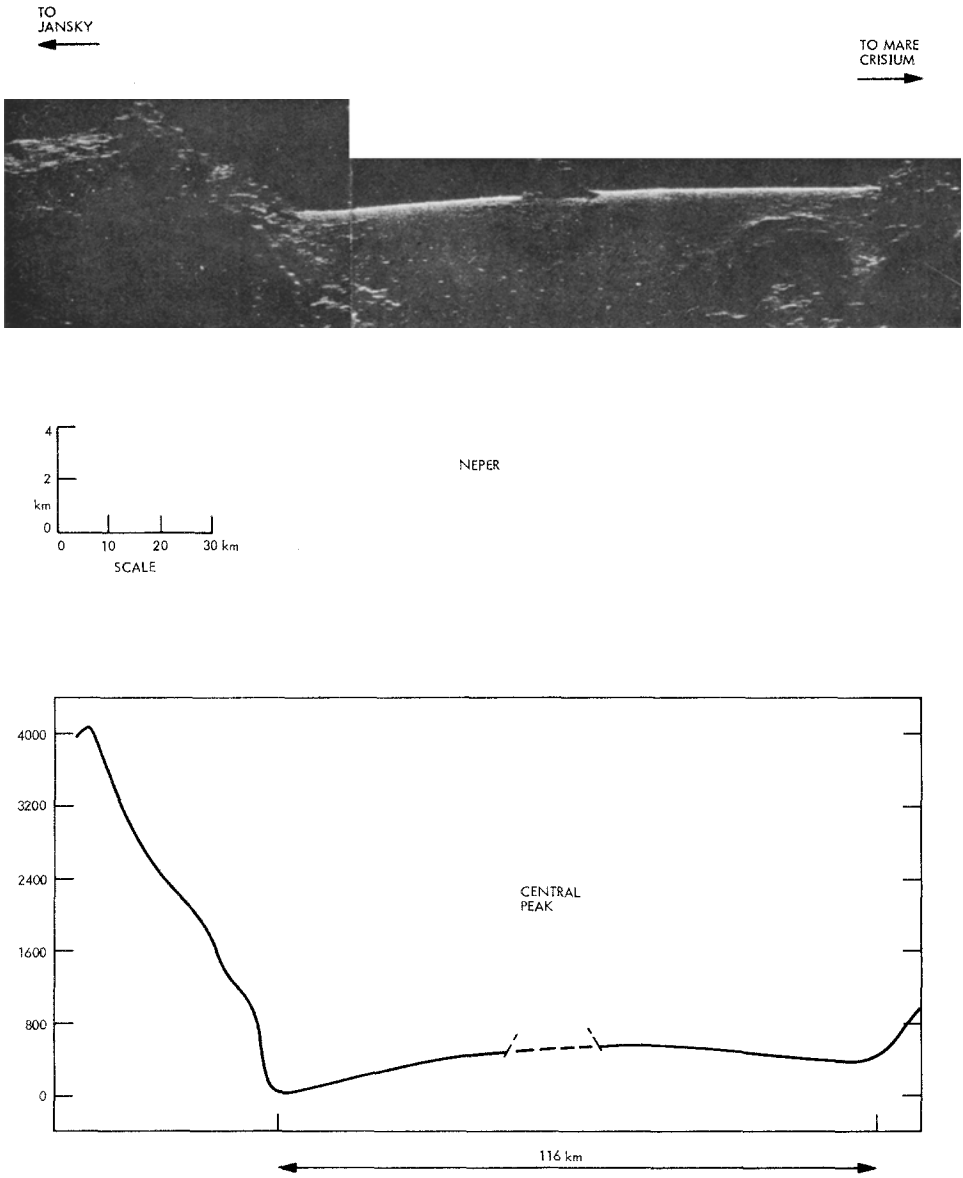

Fig. 6. Radar image and profile of Neper. Note that the east is to the left and the north is down in the image. Note also the difference in the scales. The vertical scale should only be applied to the profile and not to the cross track surface dimensions.

doming. Craters of smaller diameter (e.g., Maraldi, Love, and others) which were profiled by the ALSE radar do not exhibit the doming floor, at least not on the scale observable by the radar.

Figure 7 shows the radar and photographic imagery of Maraldi, which has a perfectly flat floor and lies 525 m below the region of Mare Tranquillitatis immediately to

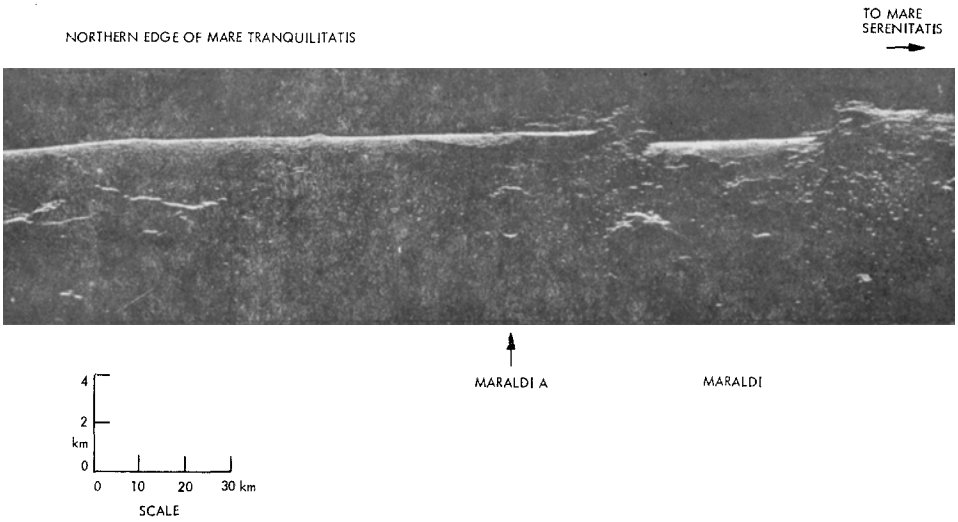

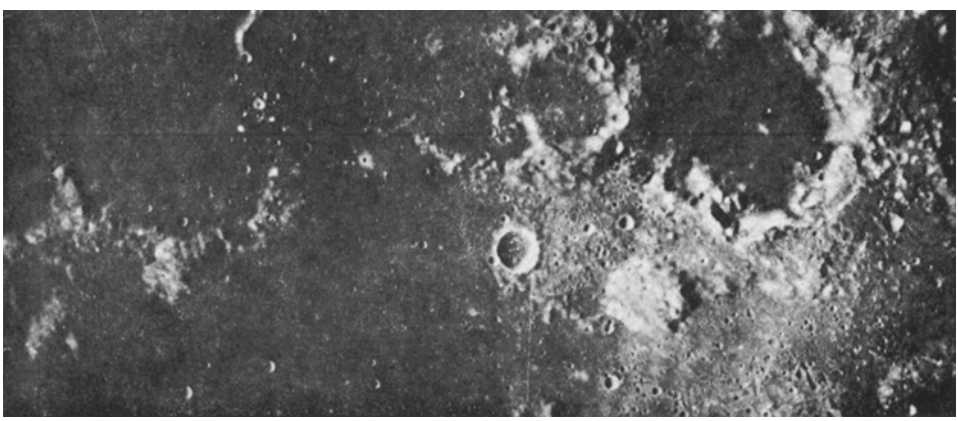

Fig. 7. Radar and photo imagery of the Maraldi region. The dash on the right of the photo corresponds to the location of the orbit, i.e., the profile seen in the radar image. Note that the east is to the left and the north is down in the two images. The vertical scale should only be applied to the profile and not to the cross track surface dimensions.

the east. This observation contradicts Bastin's (1974) statement that there seems to be no case of this kind where mare material has been insufficient to fill a given crater to the level of the adjacent maria. The explanation may lie in the relative ages of the two regions. Although it is not apparent in the photographic reproduction of Figure 7, examination of the Apollo 17 metric photography (e.g., frame 0592) shows a marked albedo difference between the interior of Maraldi and the area to the east. The Maraldi fill is noticeably darker and matches much more closely in albedo the region directly to the south. Also, Maraldi seems to contain a lower density of very small craters than the eastern area, although a detailed crater count has not been done. If these two factors are indicators of age, then Maraldi may have been filled at a later time than the region

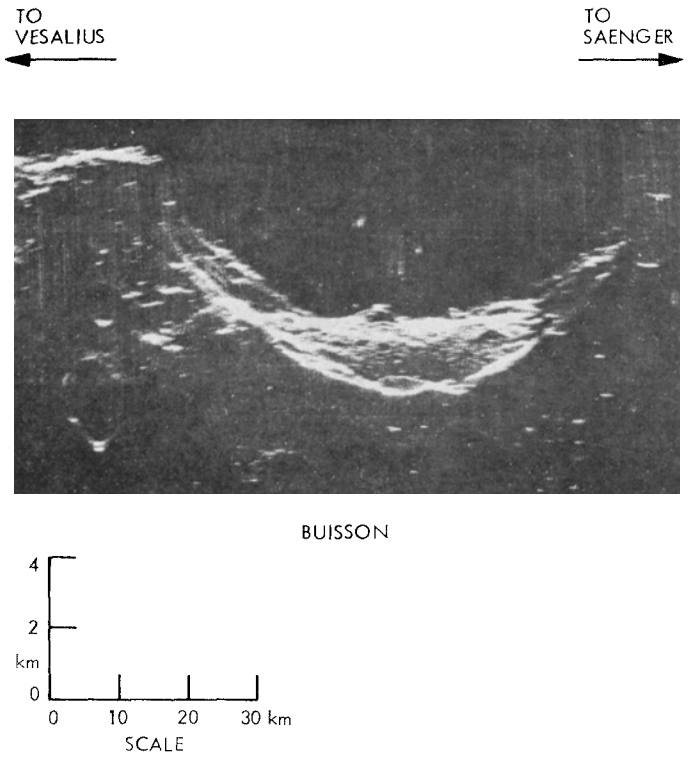

Fig. 8. Radar image of Buisson. Note that the east is to the left and the north is down in the image. The vertical scale should only be applied to the profile and not to the cross track surface dimensions.

of Tranquillitatis to the east. The laval therefore may have been subject to a lower hydrostatic pressure and filled the crater to a lower level.

Finally, we show in Figure 8 the profile of Buisson, which has a diameter of approximately 70 km. The lava flooding is less extensive. The depth/diameter ratio is equal to 0.06 versus 0.012 for Hevelius, 0.028 for Neper, and 0.036 for Maraldi. The central peak is only 425 m high.

5. Maria Profiles

During orbit 25, the Apollo 17 spacecraft also overflew Serenitatis, Northern Tranquillitatis, and Crisium. During orbit 73, it overflew southern Serenitatis and Tranquillitatis. The VHF radar data were used to generate accurate profiles along these tracks, and the results are presented in Figures 9 and 10. These profiles have been oriented for comparison with the photographs and have east to the right.

Mare Crisium: Figure 9 shows a profile across the center of Mare Crisium. The scarp depressions near the edges of the mare were measured to be 400 m deep on the western end and 520 m deep on the eastern end. An interesting note is that the shelves at the two edges of the mare are sloped toward the highland. This could be the remnant of the bottom doming due to isostatic uplift, or the fluid lava conforming to an

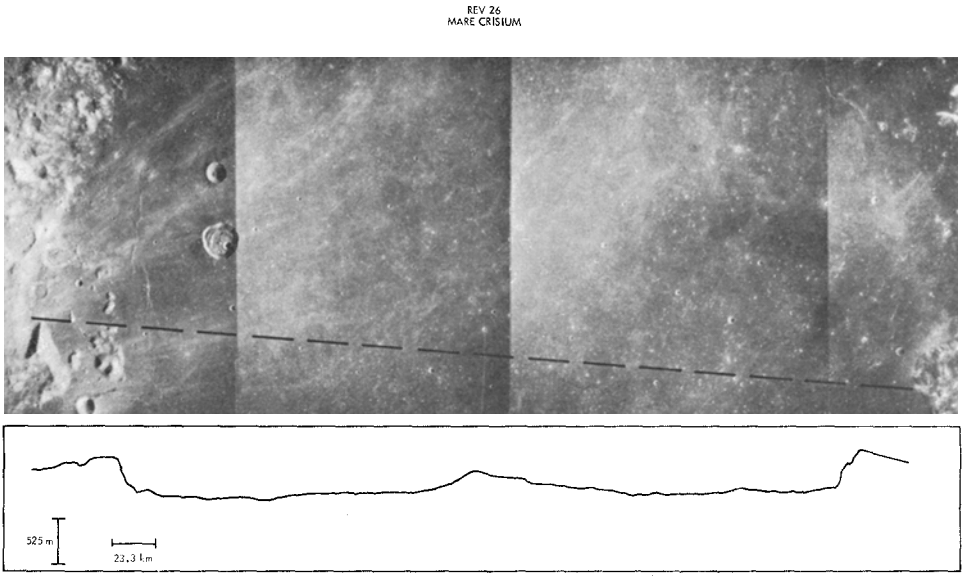

Fig. 9. Photo and radar profile of Mare Crisium. The dash line in the photo corresponds to the profile line.

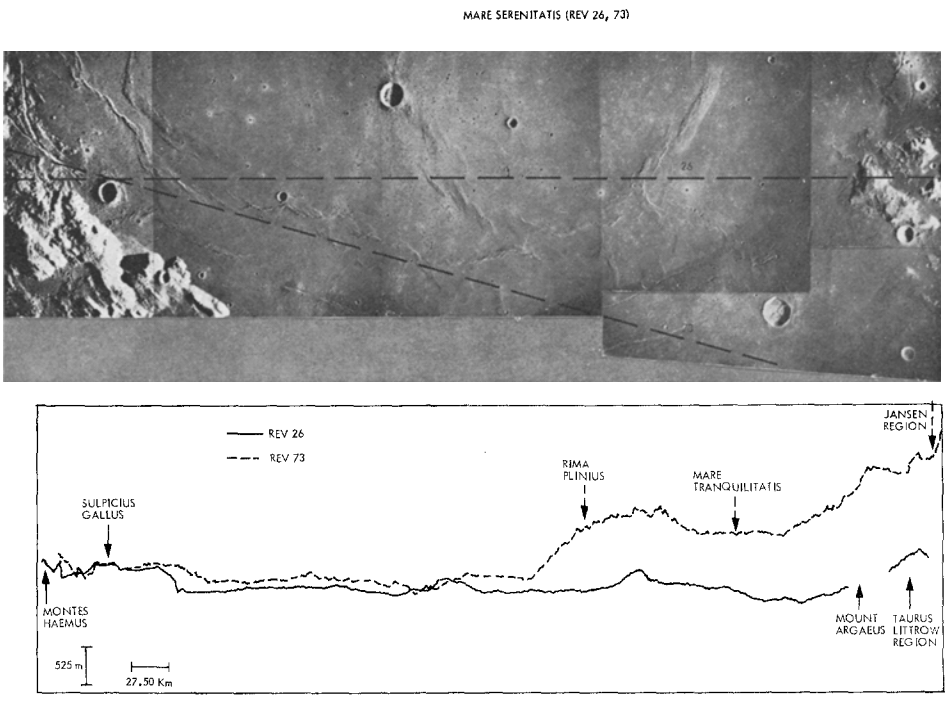

Fig. 10. Photo and radar profile of Mare Serenitatis. The dashed lines in the photo correspond to the profile lines. Note that the horizontal scale is in kilometers, not degrees of longitude. The profile taken in Revolution 26 is shown as a continuous line. The profile taken in Revolution 73 is shown as a dashed line.

equipotential surface, which might have existed before the slump of the central region. The average height of the central ridge was measured to be about 250 m with respect to the average surrounding mare level. It may represent a tensional feature due to the subsidence of the central basin or a subsurface feature which has been flooded by lava (Baldwin, 1963; Kopal, 1969). It could also represent a region of volcanic extrusion.

Mare Serenitatis: Two VHF radar profiles over Mare Serenitatis were obtained by the Apollo 17 radar (Figure 10). The first one, taken during Revolution 26, crosses the mare on an east-west line from Sulpicius Gallus to the Mons Argaeus and Taurus-Littrow regions. The second one, taken during Revolution 73, follows an oblique line from Sulpicius Gallus, across the Rima Plinius and Dawes regions, and through the northern part of Mare Tranquillitatis. The scarp depression near Sulpicius Gallus is about 260 m deep. The change in elevation at the Rima Plinius region, where Tranquillitatis lava seems to have overflown Serenitatis, is about 800 m. In general, the region of northern Tranquillitatis which was profiled seems to lie from 500 to 800 m higher than Serenitatis. The height of the ridges in central Serenitatis is 200 m, about the same as the ridge in Mare Crisium. Finally, there appears to be a slight doming in the Serenitatis region between the western scarp and the central ridges.

6. Conclusion

The ALSE radar provided accurate profiling data on a local as well as global basis. Accurate profiles of maria and large craters are an important element in the development of a theory on the formation and evolution of these lunar features. Even though most of the scientific conclusions of this paper have been qualitatively derived from photographic and gravity data, the radar measurements presented in this paper give an accurate quantitative scale. More data were taken by the ALSE radar and are under study; they are however, limited to a relatively small part of the Moon.

Acknowledgement

We would like to thank the NASA Lunar Program Office, especially Mr R. Bryson for their support during this work.

References

Arthur, D. W. G.: 1974, *Icarus* **23**, 116–133.
Baldwin, R. B.: 1963, *The Measure of the Moon*, Univ. of Chicago Press.
Baldwin R. B.: 1968, *J. Geophys. Res.* **73**, 3227–3229.
Baldwin, R. B.: 1971, *Phys. Earth Planet Interiors* **4**, 167–169.
Bastin, J. A.: 1974, *Moon* **10**, 143–162.
Brown, W. E., Jr.: 1972, *Moon* **4**, 113.
Kaula, W. m., Schubert, G., Lingenfelter, R. E., Sjogren, W. L., and Wollenhaupt, W. R.: 1974. *Proc. Fifth Lunar Sci. Conf.* **3**, 3049.
Kopal, Z.: 1969, *The Moon*, D. Reidel Publ. Co., Dordrecht, Holland.
Pike, R. J.: 1974, *Geophys. Res. Letters* **1**, 291–294.
Porcello, L., Jordan, R. L., Zelenka, J. S., Adams, G. F., Phillips, R. J., Brown, W. E., Ward, S. H , and Jackson, P. L.: 1974, *Proc. IEEE* **64**, 769–783.
Wood, Ch. A.: 1973, *Icarus* **20**, 503–506.